PROCEEDINGS B

royalsocietypublishing.org/journal/rspb

Research

Cite this article: Emery MA, Beavers KM, Van Buren EW, Batiste R, Dimos B, Pellegrino MW, Mydlarz LD. 2024 Trade-off between photosymbiosis and innate immunity influences cnidarian's response to pathogenic bacteria. *Proc. R. Soc. B* **291**: 20240428.
https://doi.org/10.1098/rspb.2024.0428

Received: 21 February 2024
Accepted: 9 August 2024

Subject Category:
Genetics and genomics

Subject Areas:
immunology, bioinformatics

Keywords:
symbiosis, innate immunity, trade-offs, mutualism, cnidarian, jellyfish

Authors for correspondence:
Madison A. Emery
e-mail: madison.emery@mavs.uta.edu
Laura D. Mydlarz
e-mail: mydlarz@uta.edu

Electronic supplementary material is available online at https://doi.org/10.6084/m9.figshare.c.7441756.

THE ROYAL SOCIETY PUBLISHING

Trade-off between photosymbiosis and innate immunity influences cnidarian's response to pathogenic bacteria

Madison A. Emery[1,2], Kelsey M. Beavers[1,3], Emily W. Van Buren[1], Renee Batiste[1], Bradford Dimos[4], Mark W. Pellegrino[1] and Laura D. Mydlarz[1]

[1]Department of Biology, University of Texas at Arlington, Arlington, TX 76019, USA
[2]Department of Integrative Biology, Michigan State University, East Lansing, MI 48824, USA
[3]Texas Advanced Computing Center, University of Texas at Austin, Austin, TX 78758, USA
[4]Department of Animal Sciences, Washington State University, Pullman, WA 99163, USA

MAE, 0009-0000-2590-1110

Mutualistic relationships with photosynthetic organisms are common in cnidarians, which form an intracellular symbiosis with dinoflagellates in the family Symbiodiniaceae. The establishment and maintenance of these symbionts are associated with the suppression of key host immune factors. Because of this, there are potential trade-offs between the nutrition that cnidarian hosts gain from their symbionts and their ability to successfully defend themselves from pathogens. To investigate these potential trade-offs, we utilized the facultatively symbiotic polyps of the upside-down jellyfish *Cassiopea xamachana* and exposed aposymbiotic and symbiotic polyps to the pathogen *Serratia marcescens*. Symbiotic polyps had a lower probability of survival following *S. marcescens* exposure. Gene expression analyses 24 hours following pathogen exposure indicate that symbiotic animals mounted a more damaging immune response, with higher levels of inflammation and oxidative stress likely resulting in more severe disruptions to cellular homeostasis. Underlying this more damaging immune response may be differences in constitutive and pathogen-induced expression of immune transcription factors between aposymbiotic and symbiotic polyps rather than broadscale immune suppression during symbiosis. Our findings indicate that in facultatively symbiotic polyps, hosting symbionts limits *C. xamachana*'s ability to survive pathogen exposure, indicating a trade-off between symbiosis and immunity that has potential implications for coral disease research.

1. Introduction

Throughout the metazoan phylogeny, several taxa have evolved photosymbiosis or mutualistic relationships with photosynthetic organisms [1]. In these mutualisms, the symbionts provide their hosts with photosynthates, which often account for the bulk of the hosts' nutrition, in exchange for nutrients such as nitrogen and the protection of being housed within the host [2,3]. Photosymbiosis is common throughout the cnidarian phylogeny, with the vast majority of symbiotic cnidarians forming an intracellular symbiosis with dinoflagellates in the family Symbiodiniaceae [2,4]. This symbiosis is best known for its vital role in coral reef ecosystems, as the nutrition provided by the symbionts allows the cnidarian hosts to live in oligotrophic environments that would otherwise be uninhabitable for them if they relied upon heterotrophy alone [5,6].

The extent to which the cnidarian host is reliant upon their symbionts for nutrition varies. This symbiosis can be obligate, as seen in tropical reef-building corals, facultative, as seen in some anemones and soft corals, or both

depending on the life stage, as seen in the scyphozoan genus *Cassiopea* [5,7–9]. While all algal symbionts are housed intracellularly in a specialized acidic organelle called the symbiosome, the cell type in which the symbionts reside is variable [2,7,8]. This is likely owing to the complex evolutionary history of the cnidarian–algal symbiosis, which has independently evolved several times [4,9,10]. Members of the classes Hexacorallia and Octocorallia, which account for the vast majority of symbiotic cnidarians, house their symbionts in the gastrodermis [2,7]. This is in contrast to the more distantly related scyphozoans whose symbionts are housed in mobile cells called amoebocytes within the mesoglea [8].

The complete mechanisms of symbiosis establishment and maintenance within cnidarians are still unknown and may vary across the independently evolved symbioses [7,11]. Recognition of the algal symbionts likely occurs via pattern recognition receptors (PRRs), though many different classes of these receptors have been implicated [11]. However, there is evidence in soft and hard corals that lectins opsonize the symbionts prior to phagocytosis [7,12–14]. Following phagocytosis, non-compatible symbionts are expelled from the symbiont-hosting cells via vomocytosis, while compatible symbionts are retained to establish their intracellular niche [15]. The establishment of compatible symbionts is strongly associated with the suppression of the cnidarian hosts' innate immune system [11,16–18]. Studies indicate that this immune suppression likely occurs via the suppression of the master immune regulator and transcription factor nuclear-factor kappa B (NFκB) or through the suppression of pathways upstream of NFκB [15,19,20]. This immune suppression persists in the symbiont-hosting cells in order to retain their symbionts [17–19].

Because symbiotic cnidarians suppress their immune systems while maintaining populations of intracellular symbionts, there is a potential trade-off between the nutrition these animals get from their symbionts and their ability to respond to pathogens. With recent increases in the frequency and severity of coral disease outbreaks, it is pertinent to understand how hosting symbionts influences cnidarians' ability to defend themselves against pathogens [21–24]. Aposymbiotic *Exaiptasia diaphana* have been shown to be less susceptible to *Serratia marcescens* infection relative to their symbiotic counterparts [25]. This species has also shown marked differences in gene expression between symbiotic and aposymbiotic animals in response to *Vibrio coralliilyticus* [26]. However, it has not been established whether immune suppression and the subsequent trade-off between symbiosis and immunity are shared across independent evolutions of the cnidarian–algal symbiosis, given the differences in the symbiont housing cell type. Therefore, we tested the infection outcomes and responses of aposymbiotic and symbiotic *Cassiopea xamachana* to the known cnidarian pathogen *S. marcescens*. *C. xamachana* are benthic jellyfish that are facultatively symbiotic in their polyp life stage [27]. This facultative symbiosis can be leveraged to disentangle the role of symbiosis in pathogen-induced stress. We found that symbiotic *C. xamachana*, similar to *E. diaphana*, are more susceptible to bacterial infection relative to their aposymbiotic counterparts. To further investigate the mechanisms of this trade-off between symbiosis and immunity, we measured their acidic organelle activity and gene expression following pathogen exposure. These data give more insights into the trade-offs between symbiosis and immunity in cnidarians by identifying core shared responses and phenomena across the independently evolved symbioses.

2. Methods

(a) Animal husbandry

C. xamachana polyps were obtained from the Dallas Children's Aquarium and maintained at 27°C in 35 ppt artificial seawater (ASW). Polyps were fed *Artemia* nauplii and given water changes twice per week. Aposymbiotic polyps were generated by maintaining animals in the dark for a minimum of two months. Polyps were considered aposymbiotic when they had fewer than 10 symbionts visible via a dissecting microscope. To confirm that our aposymbiotic polyps had vastly reduced symbiont populations relative to symbiotic polyps, we imaged 10 polyps from each symbiotic state under an enhanced green fluorescent protein (eGFP) filter using a Zeiss imager Z2 microscope. The mean fluorescence of the bell of each polyp was quantified in ImageJ (v.1.53 t) by subtracting the mean background fluorescence from the mean total fluorescence. A *t*-test was used to confirm a significant reduction in symbiont density (figure 1a; $p = 2.12 \times 10^{-7}$).

(b) Survival analysis and quantification of acidic organelle activity

Polyps were fed *Artemia* nauplii 48 h prior to the start of all experiments. *S. marcescens* was cultured at 30°C for 24 h in a general ASW media [28]. The bacteria were pelleted, washed with 0.2 µm filtered ASW and diluted down to a concentration of 10^8 colony-forming units (CFU)/ml prior to placing the polyps into the solution. Survival experiments had four treatment groups—symbiotic controls, aposymbiotic controls, symbiotic exposed and aposymbiotic exposed—and they were run at an ambient temperature of 27°C. Polyp mortality of each group was measured every 24 h following the start of the experiment. Mortality was defined as a polyp with the complete loss of bell structure. Differences in survival between treatment groups were tested using a Kaplan–Meier survival analysis using the R package survival and visualized with the R package survminer [29–31].

Acidic organelle activity was measured following 24 and 72 h of exposure to the respective treatments by incubating polyps in the dark in a solution of 5 µl ml^{-1} lysotracker red (Invitrogen L7528) in 0.2 µm filtered ASW for 30 min. Following the incubation period, animals were washed three times in 0.2 µm filtered ASW before being mounted onto slides and imaged at 5× under a red fluorescent protein (RFP) filter using a Zeiss imager Z2 microscope. Mean florescence of the bell of each polyp was quantified using Image J by subtracting the mean background fluorescence from the mean total fluorescence. A two-way ANOVA (mean fluorescence ~ symbiotic status × treatment) was used to test for differences in acidic organelle activity between treatment groups at 24 and 72 h.

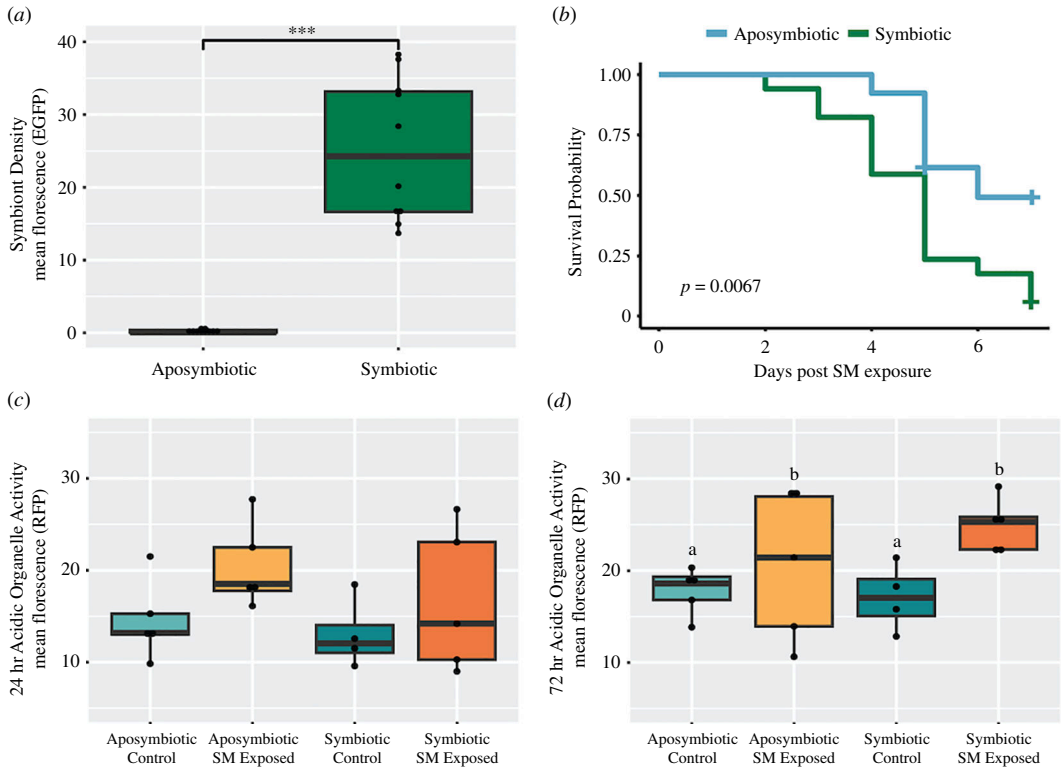

Figure 1. (*a*) Difference in symbiont density measured as mean eGFP florescence between symbiotic and aposymbiotic polyps. Points represent individual polyps' mean eGFP florescence. *** p-value < 0.001. (*b*) Kaplan–Meier survival plot comparing survival probability between symbiotic and aposymbiotic polyps following exposure to 10^8 colony-forming units (CFU) of *S. marcescens*. Crosses indicate points where individuals lived past the end of *S. marcescens* (SM) exposure. (*c,d*) Boxplots of acidic organelle activity measured as mean RFP florescence at (*c*) 24 h and (*d*) 72 h following *S. marcescens* exposure. Letters denote significantly different groups with a p-value < 0.05 resulting from a two-way ANOVA and Tukey *post hoc* test. Points represent individual polyps' mean RFP florescence.

(c) RNA extractions and sequencing

Thirty non-clonal polyps per treatment group were exposed to their respective treatment conditions for 24 h. Polyps were then pooled in groups of five for a total of six replicates per treatment group, placed into 600 µl of 1× DNA/RNA shield (Zymo: R1100) and flash frozen in liquid nitrogen. Samples were homogenized and RNA was extracted using the Zymo RNA miniprep plus kit (R1057). Extracted RNA was sent to Novogene Co. Ltd. Following quality control, 18 samples proceeded to polyA tail capture and cDNA library preparation. The cDNA libraries were then sequenced on an Illumina NovaSeq 6000 using 150 bp paired-end sequencing.

(d) Data analysis

Raw reads were trimmed using fastp (v.0.23.3) and mapped to the gene models of the *C. xamachana* draft genome using salmon (v.1.9.0) [32–34]. The corresponding proteome was annotated using both eggnogmapper (v.2.1.12) and STRING (taxon identifier STRG0A63JRD) [35,36]. Previously identified *C. xamachana* PRRs were identified in the proteome using blast [37,38]. To confirm that replicates hosted *C. xamachana's* preferred symbiont genus, *Symbiodinium*, we measured the percentage of trimmed reads per sample mapping to the *C. xamachana* gene models as well as to transcriptomes representing *Symbiodinium, Breviolium, Cladocopium* and *Durusdinium* using BBsplit v.39.01 [34,39–43]. This method of determining dominant symbiont genus has been previously utilized in reef-building corals and was verified by ITS2 data [24].

tximport was used to format the reads and correct for biases in length and GC content [44]. Outlier analyses were performed through a principal component analysis (PCA) using PCAtools and a cluster dendrogram analysis from the wgcna R package, resulting in the exclusion of three samples from downstream analysis (electronic supplementary material, figure S1) [45,46]. Following the exclusion of outliers, a second PCA was performed [46]. The loadings for principal component 1 (PC1) were then used as a variable for gene ontology (GO) enrichment analysis using gomwu [47].

Differentially expressed genes (DEGs) were called using DESeq2 with the following model: ~symbiotic status + treatment + treatment × symbiotic status [48]. The appropriate contrasts in DESeq2 were used to separate DEGs from the following comparisons: symbiotic controls versus aposymbiotic controls, aposymbiotic exposed versus aposymbiotic controls, symbiotic exposed versus symbiotic controls and symbiotic exposed versus aposymbiotic exposed. The log fold change for each of these comparisons was then used for rank-based GO enrichment analysis using gomwu.

Signed gene co-expression networks were detected using weighted gene co-expression network analysis (wgcna) with a soft power of 9 and a minimum module size of 150 (electronic supplementary material, figure S2) [45]. Modules were then correlated to treatment and symbiotic status, while each contig was correlated to treatment. Of the modules significantly correlated to any given trait or combination of traits, the most significantly correlated modules to a given trait or traits were

tested for functional enrichments. If no enrichments were found, the second most correlated module for a given trait was then tested for functional enrichments. Functional enrichments were tested using STRING against the background of all contigs with a mean expression >10 in the experiment [36]. Immune transcription factors were selected based on their significant differential expression in multiple gene expression comparisons and membership within modules most significantly correlated to a given trait or traits. A one-way ANOVA and subsequent Tukey honest significant difference (HSD) tests were run on the regularized log (rlog) normalized expression of these transcription factors to identify significant differences in expression between the four treatment groups.

3. Results

(a) Survival analysis and acidic organelle activity

Symbiotic polyps are significantly less likely to survive exposure to *S. marcescens* at a concentration of 10^8 CFU ml^{-1} relative to their aposymbiotic counterparts (Kaplan–Meier survival analysis, $p = 0.0067$) (figure 1*b*). Only 5.9% of symbiotic polyps survived exposure to the pathogen, as compared to 53.8% of aposymbiotic polyps. No mortality was observed in the symbiotic control group or the aposymbiotic control group. Acidic organelle activity did not significantly vary between any of the treatment groups 24 h following *S. marcescens* exposure (figure 1*c*). However, it significantly increased 72 h following *S. marcescens* exposure (two-way ANOVA, $p = 0.038$), with no significant effect of symbiosis on this increase (figure 1*d*).

(b) Gene expression analysis

The Symbiodiniaceae transcriptome with the highest percentage of unambiguous mapped reads was *Symbiodinium* for all replicates. This indicates that all samples were dominated by *C. xamachana's* preferred symbiont genus. An average of 11.8 million reads per replicate mapped to the *C. xamachana* gene models for an average mapping rate of 55.14% (electronic supplementary material S1). Removal of outliers resulted in 15 samples: four symbiotic control replicates, four symbiotic pathogen-exposed replicates, four aposymbiotic control replicates and three aposymbiotic pathogen-exposed replicates, for downstream analysis. After filtering genes with low expression in the dataset, the count data consisted of 16 989 expressed genes.

A PCA showed distinct grouping of the replicates by the treatment group across the first two principal components (PCs) (figure 2*a*). Notably, the symbiotic control replicates grouped most closely with aposymbiotic pathogen-exposed replicates across the first PC (PC1) (figure 2*a*). Thirty-two biological process GO terms were significantly ($p_{adj} < 0.01$) positively associated with PC1, including processes related to ion homeostasis, reactive oxygen species (ROS) metabolism and innate immunity (electronic supplementary material, S2, figure 2*b*).

Four comparisons were made during differential gene expression analysis, falling into two categories: symbiotic state comparisons and pathogen response comparisons (figure 3*a*). Symbiotic state comparisons test for differences between the symbiotic states within the same treatment groups, comparing (i) aposymbiotic controls and symbiotic controls and (ii) aposymbiotic pathogen-exposed and symbiotic pathogen-exposed. Pathogen response comparisons test the response of each symbiotic state to *S. marcescens*, comparing (iii) aposymbiotic controls and aposymbiotic pathogen-exposed, and (iv) symbiotic controls and symbiotic pathogen-exposed. There were 1157 DEGs between aposymbiotic controls and symbiotic controls, 643 of which were annotated (electronic supplementary material, S3). Of these 1157 genes, 347 were differentially expressed in both symbiotic state comparisons, regardless of exposure to *S. marcescens* (figure 3*b*).

Significant downregulation of NFκB occurred in symbiotic controls relative to aposymbiotic controls (figure 4). Several other genes associated with immune stress responses were significantly upregulated in symbiotic controls relative to their aposymbiotic counterparts, including nitric oxide synthase 1 (NOS1), interferon regulatory factor 1 (IRF1), interferon regulatory factor 4 paralog 1 (IRF4 paralog 1) and superoxide dismutase 1 (SOD1) (figure 4). Ranked GO enrichment analysis found 158 GO terms significantly upregulated and downregulated in the symbiotic controls relative to aposymbiotic controls (figure 5*a*, electronic supplementary material, S4). Several of these significantly upregulated enrichments in symbiotic controls are associated with ion transport and the nervous system (figure 5*a*). Additionally, lipid catabolism was downregulated in symbiotic controls relative to aposymbiotic controls (figure 5*a*).

When the aposymbiotic and symbiotic pathogen-exposed treatments were compared, there were 799 differentially expressed genes, 418 of which were annotated (electronic supplementary material, S3). IRF1, IRF4 *C. xamachana* paralog 1 (IRF4 paralog 1), nuclear respiratory factor 1 (NRF1) and SOD1 were all upregulated in symbiotic pathogen-exposed polyps relative to aposymbiotic polyps (figure 4). Rank-based GO enrichment analysis found evidence for a stronger immune response in symbiotic polyps relative to aposymbiotic polyps following pathogen challenge with the upregulation of GO terms indicative of immune effector secretion and oxidative stress (figure 5*a*, electronic supplementary material, S4). A total of 338 GO terms were significantly differentially expressed in this comparison (electronic supplementary material, S4).

The aposymbiotic polyps exposed to *S. marcescens* differentially expressed 746 genes relative to aposymbiotic controls, 442 of which were annotated (electronic supplementary material, S3). Many of these genes, such as IRF1, IRF4 paralog 1, SOD1 and macrophage expressed 1 (MPEG1), have functions in innate immunity (figure 4). Rank-based GO enrichment analysis found 414 differentially expressed GO terms between pathogen-exposed aposymbiotic polyps relative to aposymbiotic control polyps,

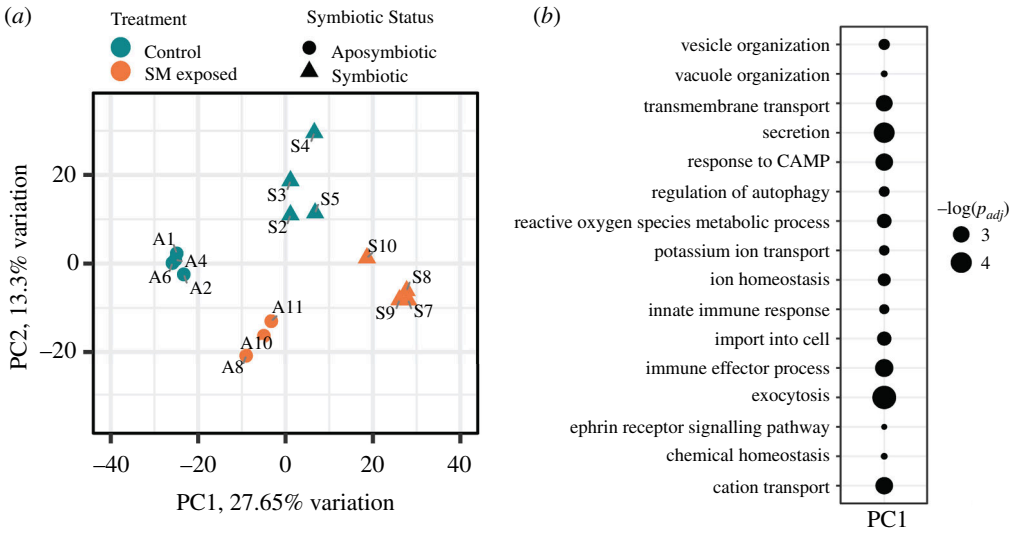

Figure 2. (*a*) PCA of rlog normalized gene expression. Teal points indicate control replicates, orange points indicate pathogen-exposed replicates, circular points indicate aposymbiotic replicates and triangular points indicate symbiotic replicates. SM, *S. marcescens*. (*b*) Rank-based gene ontology enrichments significantly positively associated with PC1. The size of each point is reflective of the −log adjusted *p*-value of its corresponding term.

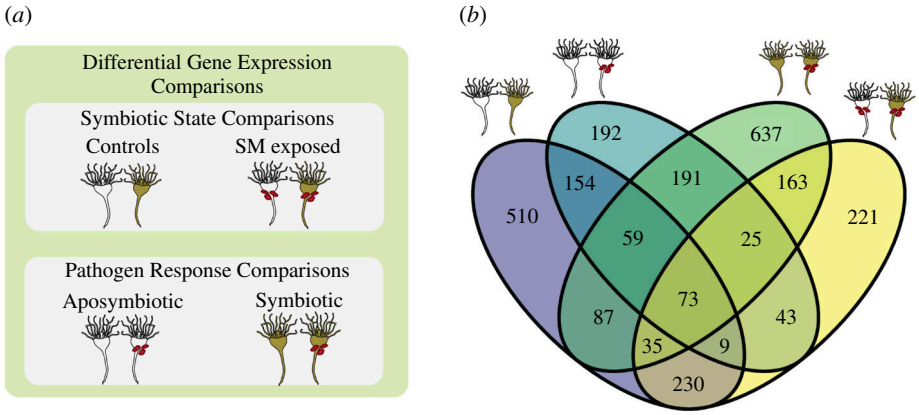

Figure 3. (*a*) Schematic of the four comparisons made during differential gene expression analysis separated into symbiotic state comparisons and pathogen response comparisons. SM, *S. marcescens*. (*b*) Venn diagram of overlapping differentially expressed genes between all differential gene expression comparisons. Specific comparisons indicated by polyp icons.

including the upregulation of terms related to phagocytosis, inflammatory immune effectors and ROS biosynthesis (figure 5*b*, electronic supplementary material, S4).

Symbiotic polyps differentially expressed 1270 genes following pathogen exposure relative to symbiotic controls, 773 of which were annotated (electronic supplementary material, S3). There were 348 overlapping genes between the aposymbiotic pathogen response comparison and the symbiotic pathogen response comparison, including the upregulation of IRF1, SOD1 and MPEG1 (figure 4). Additionally, symbiotic polyps upregulated NFκB, catalase 2 (CAT2) and NRF1 in response to *S. marcescens* (figure 4). This comparison had 515 GO enrichments. Symbiotic polyps upregulated many of the same immune stress response terms as aposymbiotic polyps in response to *S. marcescens* (figure 5*b*, electronic supplementary material, S4). However, the pathogen response of symbiotic polyps also involved the upregulation of terms indicative of oxidative stress and endoplasmic reticulum (ER) stress (figure 5*b*).

Signed weighted gene co-expression network construction resulted in 23 modules of co-expressed genes. Of these 23 modules, seven had significant correlations to treatment, four had significant correlations to symbiotic status and two had significant correlations for treatment and symbiotic status (electronic supplementary material, figure S3). The module most negatively correlated to symbiosis (Green module, $r = -0.9$, $p = 5 \times 10^{-6}$) had STRING enrichments for terms related to assembly of collagen fibrils and peptidase activity (figure 6, electronic supplementary material, S5). The module with the highest positive correlation to symbiosis (Brown module, $r = 0.92$, $p = 8 \times 10^{-7}$) did not have any significant STRING enrichments; however, the module with the next highest positive correlation to symbiosis (Grey60 module, $r = 0.59$, $p = 0.02$) was enriched for several terms related to ion transport (figure 6, electronic supplementary material, S5). The module most negatively correlated to *S. marcescens* exposure (Magenta module, $r = -0.81$, $p = 3 \times 10^{-4}$) was enriched for terms related to nitrogen metabolism. In contrast, the module most positively correlated to *S. marcescens* exposure (Black module, $r = 0.93$, $p = 7 \times 10^{-7}$) contained the transcription factor NFκB (module membership (mm) = 0.74, $p = 0.002$) and was enriched for the innate immune system and the endomembrane system (figures 6 and 7*a*). The red module was negatively correlated to both symbiosis ($r = -0.81$, $p = 3 \times 10^{-4}$) and *S. marcescens* exposure ($r = -0.63$, $p = 0.01$). This module contains IRF4 paralog 2 (mm = 0.85, $p = 6.01 \times 10^{-5}$) and was enriched for the cell cycle and cytoskeleton organization (figures 6 and 7*b*). Finally, the turquoise module was positively correlated to both symbiosis ($r = 0.67$,

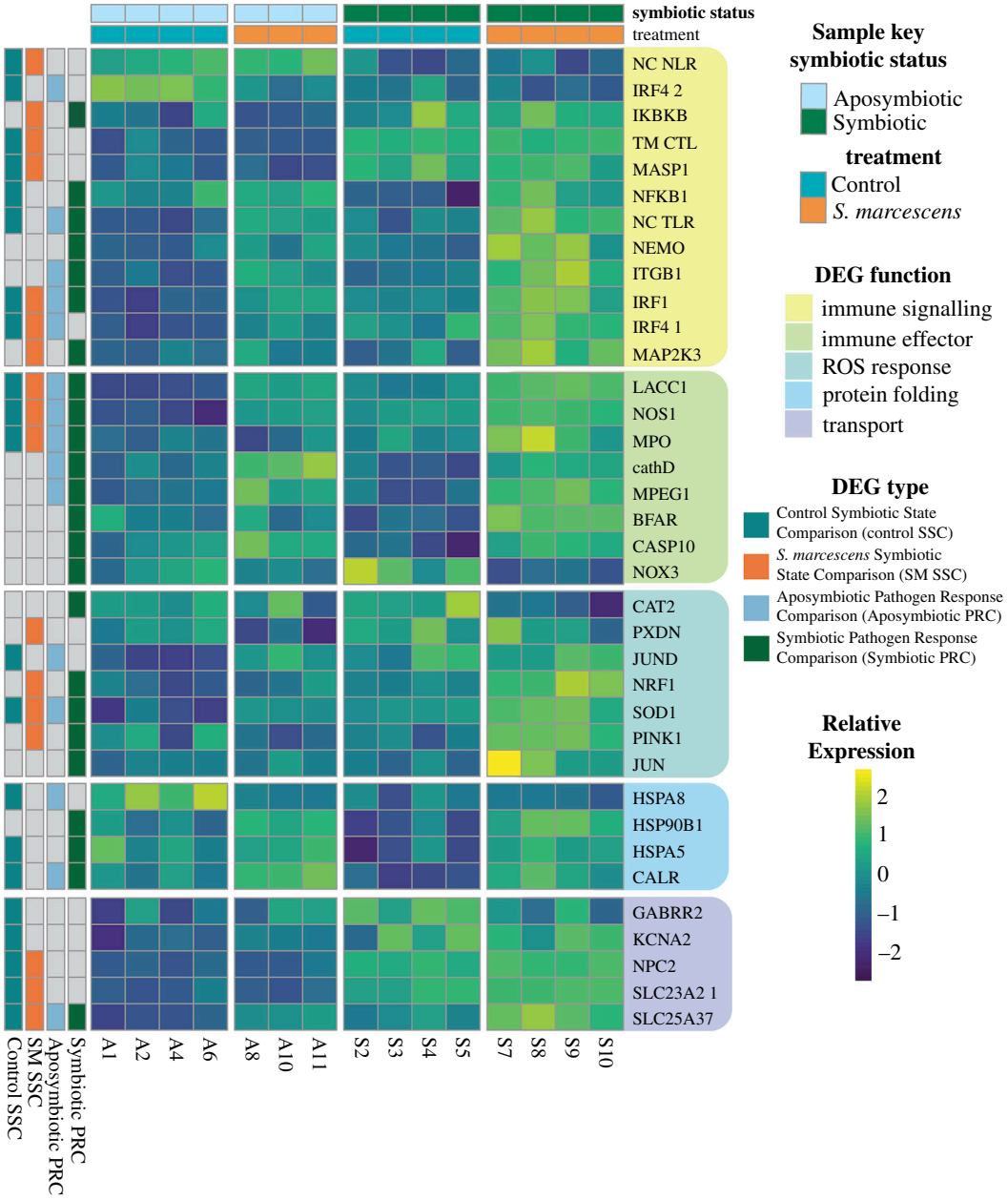

Figure 4. Heat map of select DEGs using relative rlog expression. Column key indicates symbiotic status/treatment of each section. Row key indicates which comparison(s) the gene is differentially expressed in. Rows are grouped by DEG function. abbreviations: NC NLR, non-canonical NLR; IRF4 2, IRF4 paralog 2, NC TLR-non-canonical TLR; IRF4 1, IRF4 paralog 1.

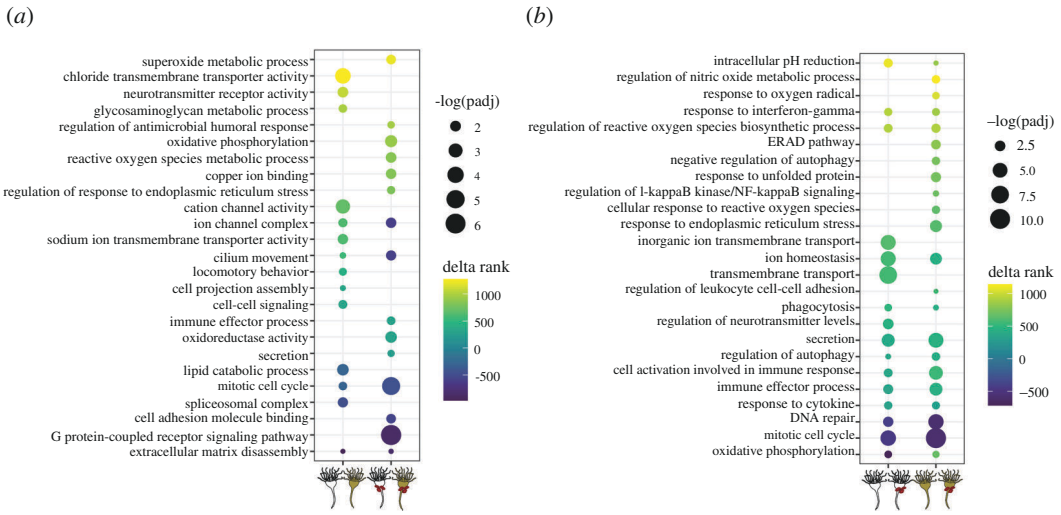

Figure 5. Curated set of rank-based gene ontology enrichments significantly differentially expressed in (*a*) symbiotic state comparisons and (*b*) pathogen response comparisons. Colour of each point indicates the delta rank of its corresponding term, while size indicates the –log-adjusted *p*-value.

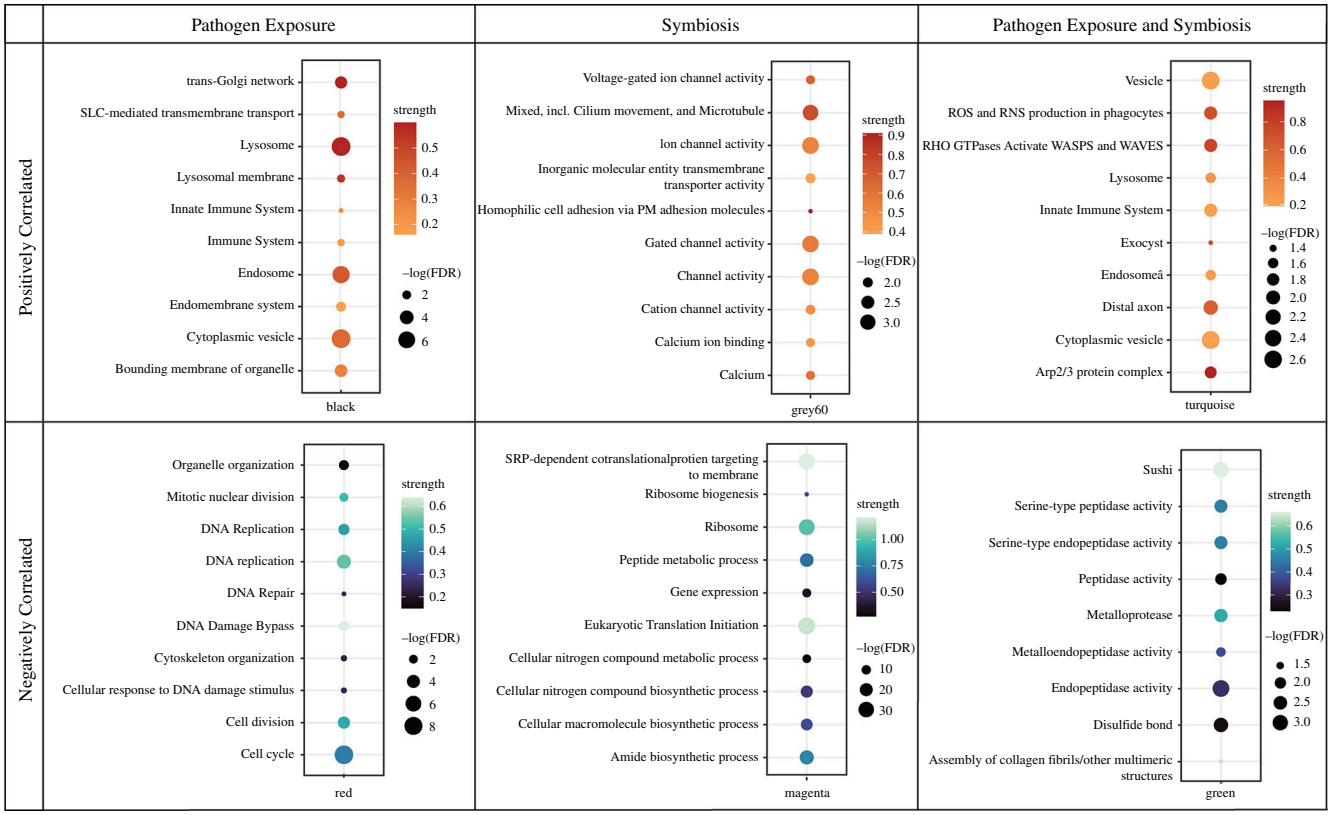

Figure 6. Curated set of STRING enrichments of WGCNA modules significantly correlated to symbiosis, pathogen exposure, or symbiosis and pathogen exposure. Colour of each point corresponds to the strength of the enrichment term, and the size of each point indicates the –log false discovery rate of the enrichment term.

$p = 0.007$) and pathogen exposure ($r = 0.76$, $p = 0.001$). This module contained two immune transcription factors, IRF1 (mm = 0.94, $p = 2.93 \times 10^{-7}$) and IRF4 paralog 1 (mm = 0.87, $p = 2.22 \times 10^{-5}$), and was enriched for the innate immune system and oxidant production (figures 6 and 7*c,d*, electronic supplementary material, S5).

4. Discussion

The lower survival of symbiotic polyps following *S. marcescens* exposure indicates the presence of a trade-off between the nutritional benefit of hosting symbionts and immunocompetence in facultatively symbiotic *C. xamachana*. We found that hosting Symbiodiniaceae alters both constitutive and pathogen-induced *C. xamachana* gene expression. Symbiosis in *C. xamachana* altered the constitutive expression of metabolism, ion transport and innate immunity. When exposed to *S. marcescens*, symbiotic *C. xamachana* upregulated a stronger ROS and immune effector response, likely disrupting protein homeostasis in the endomembrane system and leading to low survival rates. We hypothesize that differences in constitutive and pathogen-induced expression of immune transcription factors drive symbiotic polyps' greater susceptibility to bacterial pathogens.

In comparing the two control groups of our study, we found several notable differences in the constitutive expression of symbiotic and aposymbiotic *C. xamachana*. Several genes involved in transport and metabolism were differentially expressed in symbiotic animals relative to their aposymbiotic counterparts. Consistent with findings in the symbiotic sea anemone *E. diaphana*, our symbiotic controls downregulated lipid catabolism relative to their aposymbiotic counterparts. Previous studies attribute these expression changes in lipid metabolism to be indicative of increased energy stores and thus characteristic of stable symbiosis [49,50]. Interestingly, we found no evidence of constitutive shifts in symbiotic polyps' expression of nitrogen metabolism in any of our analyses. This is notable because shifts in nitrogen metabolism, specifically ammonium recycling via the glutamine synthetase/glutamate synthase system, are a well-established occurrence in symbiotic anthozoans and thought to be a mechanism of symbiont population control [9,12,17,51–54]. Isotopic studies have found that while *C. xamachana*'s symbionts have limited access to nitrate *in hospite*, they retain access to ammonium derived from heterotrophic feeding [55,56]. Our results support this finding, as GLUL, a gene responsible for the removal of ammonium by converting it to glutamine, is constitutively downregulated in symbiotic polyps. This same gene is upregulated in symbiotic *E. diaphana* and overexpressed in the symbiont-hosting cells of *Stylophora pistillata* and *Xenia* sp. [9,12,51,57]. The lack of transcriptomic signatures of constitutive changes to nitrogen metabolism in symbiotic *C. xamachana* polyps could be owing to their different symbiont-hosting cell type and their potential use of their bacterial microbiome to limit symbiont access to dissolved inorganic nitrogen [55,56].

We found extensive evidence for the constitutive differential regulation of ion transport while in a symbiotic state, with both the ranked GO enrichment analysis between control groups and the WGCNA module positively correlated to symbiosis having enrichments involving the nervous system and transmembrane ion transport. Similar expression patterns have been observed in *E. diaphana*, with many of the upregulated genes associated with ion transport (KCNA2, GAABRR2, CNTNAP4 in our study) functioning to decrease membrane excitability [51,58–60]. Several intracellular protozoan parasites cause similar

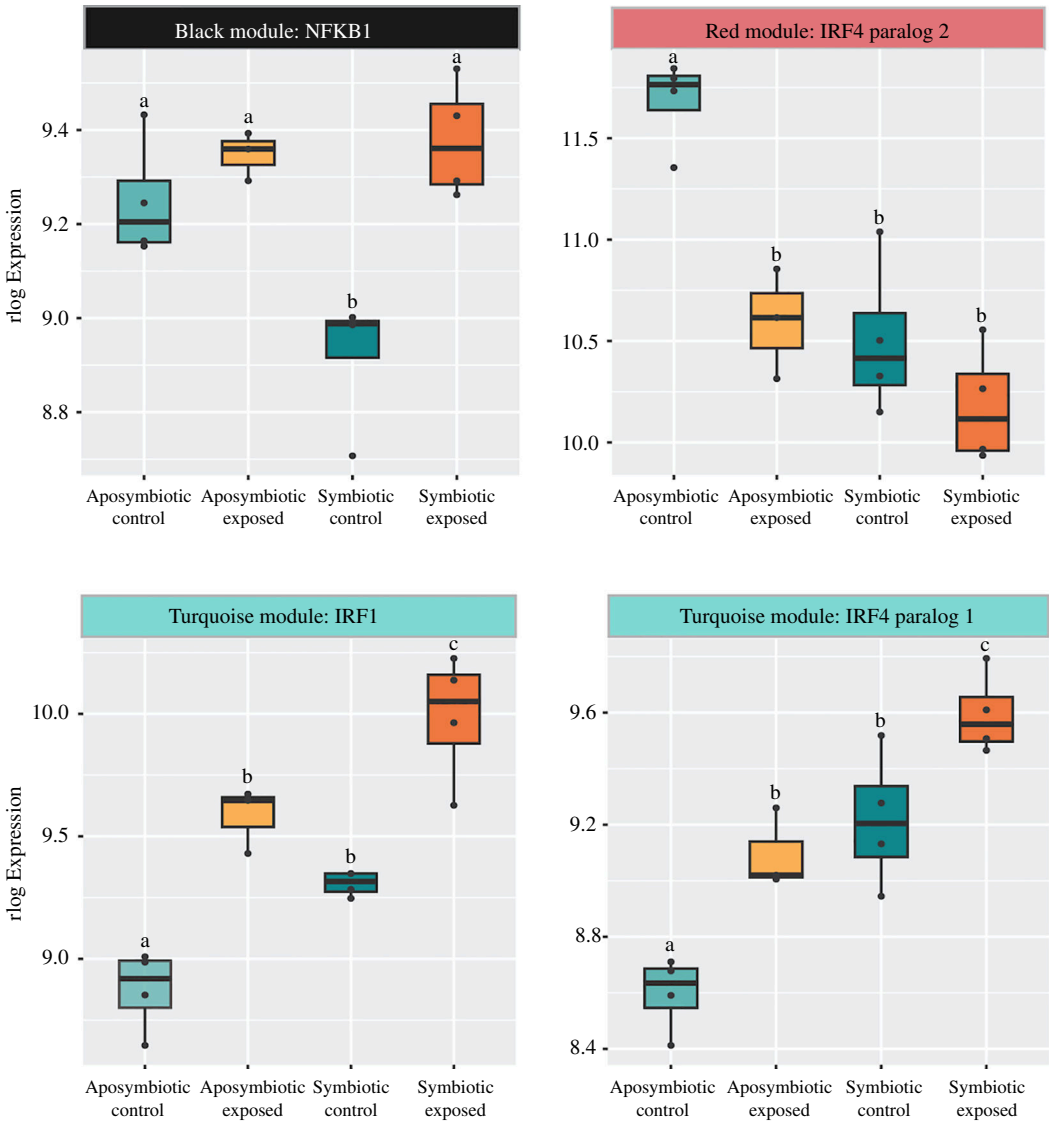

Figure 7. WGCNA module membership and box plots with the rlog expression of (*a*) NFκB, (*b*) IRF4 paralog 2, (*c*) IRF1 and (*d*) IRF4 paralog 1. Letters represent significantly different treatment groups with a p-value < 0.05 resulting from a one-way ANOVA and Tukey post hoc test. Points represent individual replicates' rlog expression.

changes to their host's ion transport, often to prevent the host cell from producing nitric oxide [61–63]. Symbiodiniaceae may employ similar strategies while residing intracellularly, as high levels of host-derived nitric oxide have been shown to lead to symbiosis breakdown [64,65]. However, nitric oxide synthase is upregulated in symbiotic controls relative to aposymbiotic controls, so the changes in expression of these ion transporters may serve a different function in the maintenance of symbionts.

Our data do not suggest that symbiotic animals have large-scale downregulation of immunity, as there were no GO terms related to immunity that were significantly differentially expressed between the two control groups. This, along with the PCA showing symbiotic controls grouping with the aposymbiotic pathogen-exposed replicates across PC1, which is enriched for genes with innate immune response GO annotations, indicates that broadscale immune suppression owing to hosting symbionts is unlikely to be driving differences in survival rates between symbiotic states as has been hypothesized in other symbiotic cnidarians [11,16]. However, we did find several immune transcription factors with significantly different constitutive expression between the symbiotic states. Two of these transcription factors, NFκB and IRF4 paralog 2, have significantly lower expression in symbiotic controls relative to aposymbiotic controls. This NFκB expression pattern has been found in symbiotic anemones [19,20]. Additionally, there is evidence that stony corals negatively regulate NFκB pathways while hosting symbionts, indicating that NFκB downregulation is a common characteristic of the cnidarian–algal symbiosis across independent evolutions of the trait [17,18].

The other two immune transcription factors differentially regulated between the control groups are IRF1 and IRF4 paralog 1, which have significantly higher expression in symbiotic controls relative to aposymbiotic controls. Interferon regulatory factors have yet to be implicated in cnidarian symbiosis, but similar to NFκB these immune transcription factors are capable of mounting pro-inflammatory immune responses [66,67]. IRF expression can be both constitutive, providing basal levels of defence against microbes, and inducible, following danger-associated molecular pattern recognition [67–69]. Our data indicate that *S. marcescens* exposure can induce IRF1 and IRF4 paralog 1 expression, but not IRF4 paralog 2. As such, aposymbiotic animals are only constitutively upregulating a single immune transcription factor with *S. marcescens*-induced expression

(NFκB), whereas symbiotic animals are constitutively upregulating two (IRF1 and IRF4 paralog 1). The differential regulation of these transcription factors may underlie why symbiotic polyps are less likely to survive *S. marcescens* exposure.

The pathogen response of symbiotic *C. xamachana* shared some similarities with aposymbiotic *C. xamachana*. Regardless of symbiotic state, *C. xamachana* polyps upregulated GO terms indicative of the secretion of immune effector proteins. One such immune effector was MPEG1, a bactericidal protein [70,71]. However, many of these same GO terms are significantly upregulated in symbiotic pathogen-exposed polyps relative to aposymbiotic pathogen-exposed polyps, indicating that symbiotic animals are likely mounting a stronger immune effector response than their aposymbiotic counterparts. This could be owing to the utilization of different pro-inflammatory immune pathways in the aposymbiotic and symbiotic pathogen responses. Both aposymbiotic and symbiotic polyps are upregulating 'response to interferon gamma' when exposed to *S. marcescens*. As cnidarians lack interferons, this GO enrichment likely suggests the upregulation of IRFs and other genes under transcriptional control of IRFs [66,72]. This is supported by both symbiotic states upregulating IRF1 in response to the pathogen. However, as symbiotic polyps have higher baseline expression of IRF1 and IRF4 paralog 1, symbiotic pathogen-exposed polyps have significantly higher expression of these transcription factors relative to aposymbiotic pathogen-exposed polyps. This is further supported by both these transcription factors belonging to the turquoise module, which is significantly positively correlated to symbiosis and *S. marcescens* exposure. Additionally, symbiotic polyps are upregulating the GO term 'regulation of IκBK/NFκB signaling' in response to *S. marcescens* as well as NFκB and one of its activators, NFκB essential modulator (NEMO). However, symbiotic polyps are also upregulating IκBKB, the inhibitor of NFκB, in response to *S. marcescens*. As NFκB is often a component of the initial immune signalling following the introduction of a stressor, this could suggest that at 24 h following *S. marcescens* exposure, symbiotic polyps are transitioning to different immune stress response pathways [73,74].

Stronger pro-inflammatory immune signalling in symbiotic polyps relative to aposymbiotic polyps could explain why gene expression signatures of oxidative stress are higher in pathogen-exposed symbiotic polyps relative to their aposymbiotic counterparts [75]. While the pathogen response of both symbiotic states included the upregulation of the GO term 'regulation of ROS biosynthetic process', only the symbiotic pathogen response included the upregulation of GO terms associated with responding to ROS. Additionally, the turquoise module, which is positively correlated to both pathogen exposure and symbiosis, is enriched for oxidant production. Higher levels of oxidants in pathogen-exposed symbiotic polyps are further supported by their significantly higher expression of the antioxidant SOD1 and the oxidative stress transcription factor NRF1 relative to pathogen-exposed aposymbiotic polyps [76,77]. Pro-inflammatory factors can induce ROS production directly and indirectly [78,79]. Higher demands for immune effector secretion can result in the upregulation of oxidative phosphorylation during immune responses [80]. The upregulation of oxidative phosphorylation in symbiotic pathogen-exposed polyps relative to their aposymbiotic counterparts may be another contributor to the higher transcriptional signatures of oxidative stress in the symbiotic pathogen response. Together, the stronger upregulation of immune effector responses, oxidative stress responses and oxidative phosphorylation in symbiotic polyps indicates that their immune response to *S. marcescens* likely results in more severe disruptions to cellular homeostasis relative to aposymbiotic polyps [78–80].

Our gene expression data indicate that symbiotic polyps experience disruptions to endomembrane system homeostasis and the protein folding environment within the cell. Oxidative stress, high secretory demand and immune effector proteins are all capable of disrupting the protein folding environment within the ER and are more highly upregulated in symbiotic pathogen-exposed replicates relative to aposymbiotic pathogen-exposed replicates [81–83]. Symbiotic polyps upregulated both the endoplasmic-reticulum-associated protein degradation (ERAD) pathway and an unfolded protein response (UPR). These pathways are both indicative of disruptions to protein homeostasis and ER stress [84]. The ERAD pathway is responsible for removing misfolded or unfolded proteins from the ER. If these misfolded and/or unfolded proteins accumulate, they will trigger the UPR [84,85]. In response to the accumulation of misfolded and/or unfolded proteins, the UPR reduces protein synthesis and upregulates chaperonins to attempt to refold or repair the misfolded proteins [81,84]. Any proteins unable to be folded are degraded via either autophagy or the ERAD pathway [81,82,84]. If the cell is unable to correctly repair or refold its proteins or the misfolded proteins accumulate and are not able to be degraded, the UPR transitions into a cell death pathway [82,86]. Given that symbiotic polyps have considerably more disruptions to protein homeostasis at 24 h following *S. marcescens* exposure, they likely are transitioning to cell death pathways sooner than aposymbiotic polyps, resulting in lower survival.

Differential expression of genes associated with autophagy is a common component of cnidarian immune responses, particularly at relatively early timepoints following pathogen exposure or in disease-resistant coral species that are not as severely impacted by a given pathogen [87,88]. In the context of innate immunity, autophagy is cytoprotective and anti-inflammatory, counteracting the damage that secreted inflammatory factors can cause to mitochondria and the endomembrane system [89]. Both symbiotic and aposymbiotic polyps significantly changed their regulation of autophagy and had increased acidic organelle activity following exposure to *S. marcescens*. However, given the signatures of higher oxidative stress and ER stress in symbiotic polyps, it is likely that upregulation of autophagy is insufficient to counteract the damage caused by their immune response, resulting in the negative regulation of autophagy and transition to cell death pathways [86,89].

5. Conclusions

Together, our data demonstrate that there is a trade-off between photosymbiosis and immunocompetence in the facultatively symbiotic polyps of *C. xamachana*. Underlying this trade-off may be the differential regulation of immune transcription factors both constitutively and in response to *S. marcescens* exposure rather than broadscale immune suppression in symbiotic animals. Symbiotic *C. xamachana* mount a stronger and more damaging immune response following pathogen exposure, resulting in higher levels of oxidative stress, greater disruptions to cellular homeostasis and ultimately decreased survival rates. The

trade-off between symbiosis and immunity seems to be shared across independent evolutions of facultative cnidarian–algal symbiosis, as *E. diaphana* are also more susceptible to *S. marcescens* in a symbiotic state [25]. There likely are more complexities to the nutritional aspect of this trade-off, as starvation has been shown to influence cnidarian immune gene expression [25,90]. With the expanding threat of disease to coral reef ecosystems, this trade-off could be a major factor in coral disease susceptibility and dysbiosis via bleaching or nutrient pollution. The cost of hosting symbionts should be investigated further and potentially incorporated into the paradigms of coral disease research [21,91].

Ethics. This work did not require ethical approval from a human subject or animal welfare committee.

Data accessibility. Microscopy images, survival data, all shell scripts, and all R code used are available in the Data Dryad Repository [92]. All raw sequence data and associated sample metadata are available on the NCBI SRA database (BioProject ID PRJNA1077944). Publicly available data used in this study include the draft *C. xamachana* genome gene models (https://mycocosm.jgi.doe.gov/Casxa1/Casxa1.home.html).

Supplementary material is available online [93].

Declaration of AI use. We have not used AI-assisted technologies in creating this article.

Authors' contributions. M.A.E.: conceptualization, data curation, formal analysis, funding acquisition, investigation, methodology, project administration, software, validation, visualization, writing—original draft, writing—review and editing; K.M.B.: methodology, software, writing—review and editing; E.W.V.B.: formal analysis, software, writing—review and editing; R.B.: formal analysis, writing—review and editing; B.D.: conceptualization, methodology, writing—review and editing; M.W.P.: conceptualization, writing—review and editing; L.M.: conceptualization, funding acquisition, supervision, writing—review and editing.

All authors gave final approval for publication and agreed to be held accountable for the work performed therein.

Conflict of interest declaration. We declare we have no competing interests.

Funding. This study was funded by the University of Texas at Arlington Phi Sigma research grant to M.A.E., the Society of Integrative and Comparative Biology John Pearse Research Award to M.A.E., and the NSF EEID (award number 2109622) to L.D.M.

Acknowledgements. The authors would like to thank Martin Nicholas for his assistance with the survival assays, Dr. Jeffery Demuth for his input on bioinformatic methods, and Mydlarz lab members Hannah Swain and Daniela Gutierrez for their input and support. Additionally, we thank the anonymous reviewers for their insight.

References

1. Melo Clavijo J, Donath A, Serôdio J, Christa G. 2018 Polymorphic adaptations in metazoans to establish and maintain photosymbioses. Biol. Rev. Camb. Philos. Soc. **93**, 2006–2020. (doi:10.1111/brv.12430)
2. Davy SK, Allemand D, Weis VM. 2012 Cell biology of cnidarian-dinoflagellate symbiosis. *Microbiol. Mol. Biol. Rev.* **76**, 229–261. (doi:10.1128/MMBR.05014-11)
3. Dean AD, Minter EJA, Sørensen MES, Lowe CD, Cameron DD, Brockhurst MA, Wood AJ. 2016 Host control and nutrient trading in a photosynthetic symbiosis. *J. Theor. Biol.* **405**, 82–93. (doi:10.1016/j.jtbi.2016.02.021)
4. Kayal E, Bentlage B, Pankey MS, Ohdera AH, Medina M, Plachetzki DC, Collins AG, Ryan JF. 2018 Phylogenomics provides a robust topology of the major cnidarian lineages and insights on the origins of key organismal traits. *BMC Evol. Biol.* **18**, 68. (doi:10.1186/s12862-018-1142-0)
5. Roth MS. 2014 The engine of the reef: photobiology of the coral–algal symbiosis. *Front. Microbiol.* **5**, 422. (doi:10.3389/fmicb.2014.00422)
6. Muscatine L, Ferrier-Pagès C, Blackburn A, Gates RD, Baghdasarian G, Allemand D. 1998 Cell-specific density of symbiotic dinoflagellates in tropical anthozoans. *Coral Reefs* **17**, 329–337. (doi:10.1007/s003380050133)
7. Jacobovitz MR, Hambleton EA, Guse A. 2023 Unlocking the complex cell biology of coral–dinoflagellate symbiosis: a model systems approach. *Annu. Rev. Genet.* **57**, 411–434. (doi:10.1146/annurev-genet-072320-125436)
8. Djeghri N, Pondaven P, Stibor H, Dawson MN. 2019 Review of the diversity, traits, and ecology of zooxanthellate jellyfishes. *Mar. Biol.* **166**, 147. (doi:10.1007/s00227-019-3581-6)
9. Levy S, Elek A, Grau-Bové X, Menéndez-Bravo S, Iglesias M, Tanay A, Mass T, Sebé-Pedrós A. 2021 A stony coral cell atlas illuminates the molecular and cellular basis of coral symbiosis, calcification, and immunity. *Cell* **184**, 2973–2987. (doi:10.1016/j.cell.2021.04.005)
10. Van Oppen MJH, Mieog JC, Sánchez CA, Fabricius KE. 2005 Diversity of algal endosymbionts (Zooxanthellae) in octocorals: the roles of geography and host relationships. *Mol. Ecol.* **14**, 2403–2417. (doi:10.1111/j.1365-294X.2005.02545.x)
11. Mansfield KM, Gilmore TD. 2019 Innate immunity and cnidarian-symbiodiniaceae mutualism. *Dev. Comp. Immunol.* **90**, 199–209. (doi:10.1016/j.dci.2018.09.020)
12. Hu M, Zheng X, Fan CM, Zheng Y. 2020 Lineage dynamics of the endosymbiotic cell type in the soft coral *Xenia*. *Nature* **582**, 534–538. (doi:10.1038/s41586-020-2385-7)
13. Hu M, Bai Y, Zheng X, Zheng Y. 2023 Coral–algal endosymbiosis characterized using RNAi and single-cell RNA-seq. *Nat. Microbiol.* **8**, 1240–1251. (doi:10.1038/s41564-023-01397-9)
14. Kvennefors ECE, Leggat W, Hoegh-Guldberg O, Degnan BM, Barnes AC. 2008 An ancient and variable mannose-binding lectin from the coral *Acropora millepora* binds both pathogens and symbionts. *Dev. Comp. Immunol.* **32**, 1582–1592. (doi:10.1016/j.dci.2008.05.010)
15. Jacobovitz MR, Rupp S, Voss PA, Maegele I, Gornik SG, Guse A. 2021 Dinoflagellate symbionts escape vomocytosis by host cell immune suppression. *Nat. Microbiol.* **6**, 769–782. (doi:10.1038/s41564-021-00897-w)
16. Fuess LE, Palacio-Castro AM, Butler CC, Baker AC, Mydlarz LD. Increased algal symbiont density reduces host immunity in a threatened Caribbean coral species, *Orbicella faveolata*. *Front. Ecol. Evol.* **8**. (doi:10.3389/fevo.2020.572942)
17. Rivera HE, Davies SW. 2021 Symbiosis maintenance in the facultative coral, *Oculina arbuscula*, relies on nitrogen cycling, cell cycle modulation, and immunity. *Sci. Rep.* **11**, 21226. (doi:10.1038/s41598-021-00697-6)
18. Mohamed AR, Andrade N, Moya A, Chan CX, Negri AP, Bourne DG, Ying H, Ball EE, Miller DJ. 2020 Dual RNA-sequencing analyses of a coral and its native symbiont during the establishment of symbiosis. *Mol. Ecol.* **29**, 3921–3937. (doi:10.1111/mec.15612)
19. Mansfield KM *et al*. 2017 Transcription factor NF-κB is modulated by symbiotic status in a sea anemone model of cnidarian bleaching. *Sci. Rep.* **7**, 16025. (doi:10.1038/s41598-017-16168-w)
20. Wolfowicz I, Baumgarten S, Voss PA, Hambleton EA, Voolstra CR, Hatta M, Guse A. 2016 *Aiptasia* sp. larvae as a model to reveal mechanisms of symbiont selection in cnidarians. *Sci. Rep.* **6**, 32366. (doi:10.1038/srep32366)

21. Bourne DG, Garren M, Work TM, Rosenberg E, Smith GW, Harvell CD. 2009 Microbial disease and the coral holobiont. *Trends Microbiol.* **17**, 554–562. (doi:10.1016/j.tim.2009.09.004)
22. Tracy AM, Pielmeier ML, Yoshioka RM, Heron SF, Harvell CD. 2019 Increases and decreases in marine disease reports in an era of global change. *Proc. R. Soc. B* **286**, 20191718. (doi:10.1098/rspb.2019.1718)
23. Papke E *et al*. 2024 Stony coral tissue loss disease: a review of emergence, impacts, etiology, diagnostics, and intervention. *Front. Mar. Sci.* **10**. (doi:10.3389/fmars.2023.1321271)
24. Beavers KM *et al*. 2023 Stony coral tissue loss disease induces transcriptional signatures of *in situ* degradation of dysfunctional symbiodiniaceae. *Nat. Commun.* **14**, 2915. (doi:10.1038/s41467-023-38612-4)
25. Valadez-Ingersoll M, Aguirre Carrión PJ, Bodnar CA, Desai NA, Gilmore TD, Davies SW. 2023 Nutrient deprivation differentially affects gene expression, immunity, and pathogen susceptibility across symbiotic states in a model cnidarian. *bioRxiv* 2023.07.30.551141. (doi:10.1101/2023.07.30.551141)
26. Roesel CL, Vollmer SV. 2019 Differential gene expression analysis of symbiotic and aposymbiotic *Exaiptasia* anemones under immune challenge with *Vibrio coralliilyticus*. *Ecol. Evol.* **9**, 8279–8293. (doi:10.1002/ece3.5403)
27. Ohdera AH *et al*. 2018 Upside-down but headed in the right direction: review of the highly versatile *Cassiopea xamachana* system. *Front. Ecol. Evol.* **6**, 35. (doi:10.3389/fevo.2018.00035)
28. Ushijima B, Smith A, Aeby GS, Callahan SM. 2012 *Vibrio owensii* induces the tissue loss disease *Montipora* white syndrome in the Hawaiian reef coral *Montipora capitata*. *PLoS One* **7**, e46717. (doi:10.1371/journal.pone.0046717)
29. Therneau TM, Grambsch PM. 2000 *Modeling survival data: extending the Cox model*. (eds K Dietz, M Gail, K Krickeberg, J Samet, A Tsiatis). New York, NY: Springer. (doi:10.1007/978-1-4757-3294-8)
30. Therneau T. 2023 A package for survival analysis in R. See https://CRAN.R-project.org/package=survival.
31. Kassambara A, Kosinski M, Biecek P. *survminer: Drawing Survival Curves using 'ggplot2*. See https://CRAN.R-project.org/package=survminer.
32. Chen S, Zhou Y, Chen Y, Gu J. 2018 Fastp: an ultra-fast all-in-one FASTQ preprocessor. *Bioinformatics* **34**, i884–i890. (doi:10.1093/bioinformatics/bty560)
33. Patro R, Duggal G, Love MI, Irizarry RA, Kingsford C. 2017 Salmon provides fast and bias-aware quantification of transcript expression. *Nat. Methods* **14**, 417–419. (doi:10.1038/nmeth.4197)
34. Ohdera AH. Home - Cassiopea xamachana. See https://mycocosm.jgi.doe.gov/Casxa1/Casxa1.home.html.
35. Cantalapiedra CP, Hernández-Plaza A, Letunic I, Bork P, Huerta-Cepas J. 2021 EggNOG-mapper v2: functional annotation, orthology assignments, and domain prediction at the metagenomic scale. *Mol. Biol. Evol.* **38**, 5825–5829. (doi:10.1093/molbev/msab293)
36. Szklarczyk D *et al*. 2023 The STRING database in 2023: protein–protein association networks and functional enrichment analyses for any sequenced genome of interest. *Nucleic Acids Res.* **51**, D638–D646. (doi:10.1093/nar/gkac1000)
37. Emery MA, Dimos BA, Mydlarz LD. 2021 Cnidarian pattern recognition receptor repertoires reflect both phylogeny and life history traits. *Front. Immunol.* **12**, 689463. (doi:10.3389/fimmu.2021.689463)
38. Altschul SF, Gish W, Miller W, Myers EW, Lipman DJ. 1990 Basic local alignment search tool. *J. Mol. Biol.* **215**, 403–410. (doi:10.1016/S0022-2836(05)80360-2)
39. Bayer T, Aranda M, Sunagawa S, Yum LK, Desalvo MK, Lindquist E, Coffroth MA, Voolstra CR, Medina M. 2012 *Symbiodinium* transcriptomes: genome insights into the dinoflagellate symbionts of reef-building corals. *PLoS One* **7**, e35269. (doi:10.1371/journal.pone.0035269)
40. Bushnell B. 2014 *bbmap: A fast, accurate, splice-aware aligner*. Lawrence Berkeley national lab. See https://www.osti.gov/biblio/1241166.
41. Parkinson JE, Baumgarten S, Michell CT, Baums IB, LaJeunesse TC, Voolstra CR. 2016 Gene expression variation resolves species and individual strains among coral-associated dinoflagellates within the genus *Symbiodinium*. *Genome Biol. Evol.* **8**, 665–680. (doi:10.1093/gbe/evw019)
42. Davies SW, Ries JB, Marchetti A, Castillo KD. 2018 *Symbiodinium* functional diversity in the coral *Siderastrea siderea* is influenced by thermal stress and reef environment, but not ocean acidification. *Front. Mar. Sci.* **5**, 150. (doi:10.3389/fmars.2018.00150)
43. Bellantuono AJ, Dougan KE, Granados-Cifuentes C, Rodriguez-Lanetty M. 2019 Free-living and symbiotic lifestyles of a thermotolerant coral endosymbiont display profoundly distinct transcriptomes under both stable and heat stress conditions. *Mol. Ecol.* **28**, 5265–5281. (doi:10.1111/mec.15300)
44. Soneson C, Love MI, Robinson MD. 2015 Differential analyses for RNA-seq: transcript-level estimates improve gene-level inferences. *F1000Res.* **4**, 1521. (doi:10.12688/f1000research.7563.2)
45. Langfelder P, Horvath S. 2008 WGCNA: an R package for weighted correlation network analysis. *BMC Bioinformatics* **9**, 559. (doi:10.1186/1471-2105-9-559)
46. Blighe K, Lun A. 2022 *PCAtools: Everything Principal Components Analysis R package version 2.10.0*. See https://github.com/kevinblighe/PCAtools.
47. Wright RM, Aglyamova GV, Meyer E, Matz MV. 2015 Gene expression associated with white syndromes in a reef building coral, *Acropora hyacinthus*. *BMC Genomics* **16**, 371. (doi:10.1186/s12864-015-1540-2)
48. Love MI, Huber W, Anders S. 2014 Moderated estimation of fold change and dispersion for RNA-seq data with DESeq2. *Genome Biol.* **15**, 550. (doi:10.1186/s13059-014-0550-8)
49. Matthews JL, Crowder CM, Oakley CA, Lutz A, Roessner U, Meyer E, Grossman AR, Weis VM, Davy SK. 2017 Optimal nutrient exchange and immune responses operate in partner specificity in the cnidarian-dinoflagellate symbiosis. *Proc. Natl Acad. Sci. USA* **114**, 13194–13199. (doi:10.1073/pnas.1710733114)
50. Matthews JL, Oakley CA, Lutz A, Hillyer KE, Roessner U, Grossman AR, Weis VM, Davy SK. 2018 Partner switching and metabolic flux in a model cnidarian–dinoflagellate symbiosis. *Proc. R. Soc. B* **285**, 20182336. (doi:10.1098/rspb.2018.2336)
51. Cui G, Liew YJ, Li Y, Kharbatia N, Zahran NI, Emwas AH, Eguiluz VM, Aranda M. 2019 Host-dependent nitrogen recycling as a mechanism of symbiont control in aiptasia. *PLoS Genet.* **15**, e1008189. (doi:10.1371/journal.pgen.1008189)
52. Cui G *et al*. 2023 Molecular insights into the darwin paradox of coral reefs from the sea anemone *Aiptasia*. *Sci. Adv.* **9**, eadf7108. (doi:10.1126/sciadv.adf7108)
53. Xiang T, Lehnert E, Jinkerson RE, Clowez S, Kim RG, DeNofrio JC, Pringle JR, Grossman AR. 2020 Symbiont population control by host-symbiont metabolic interaction in symbiodiniaceae-cnidarian associations. *Nat. Commun.* **11**, 108. (doi:10.1038/s41467-019-13963-z)
54. DiRoberts L, Dudek A, Ray N, Fulweiler R, Rotjan R. 2021 Testing assumptions of nitrogen cycling between a temperate, model coral host and its facultative symbiont: symbiotic contributions to dissolved inorganic nitrogen assimilation. *Mar. Ecol. Prog. Ser.* **670**, 61–74. (doi:10.3354/meps13731)
55. Lyndby NH, Rädecker N, Bessette S, Søgaard Jensen LH, Escrig S, Trampe E, Kühl M, Meibom A. 2020 Amoebocytes facilitate efficient carbon and nitrogen assimilation in the *Cassiopea*-symbiodiniaceae symbiosis. *Proc. R. Soc. B* **287**, 20202393. (doi:10.1098/rspb.2020.2393)
56. Röthig T, Puntin G, Wong JCY, Burian A, McLeod W, Baker DM. 2021 Holobiont nitrogen control and its potential for eutrophication resistance in an obligate photosymbiotic jellyfish. *Microbiome* **9**, 127. (doi:10.1186/s40168-021-01075-0)
57. Eelen G *et al*. 2018 Role of glutamine synthetase in angiogenesis beyond glutamine synthesis. *Nature* **561**, 63–69. (doi:10.1038/s41586-018-0466-7)
58. Shen W, Hernandez-Lopez S, Tkatch T, Held JE, Surmeier DJ. 2004 Kv1.2-containing K+ channels regulate subthreshold excitability of striatal medium spiny neurons. *J. Neurophysiol.* **91**, 1337–1349. (doi:10.1152/jn.00414.2003)

59. Geng Y *et al*. 2012 Structure and functional interaction of the extracellular domain of human GABA(B) receptor GBR2. *Nat. Neurosci.* **15**, 970–978. (doi:10.1038/nn.3133)
60. Karayannis T *et al*. 2014 Cntnap4 differentially contributes to gabaergic and dopaminergic synaptic transmission. *Nature* **511**, 236–240. (doi:10.1038/nature13248)
61. Staines HM *et al*. 2007 Electrophysiological studies of malaria parasite-infected erythrocytes: current status. *Int. J. Parasitol.* **37**, 475–482. (doi:10.1016/j.ijpara.2006.12.013)
62. Camacho M, Forero ME, Fajardo C, Niño A, Morales P, Campos H. 2008 *Leishmania amazonensis* infection may affect the ability of the host macrophage to be activated by altering their outward potassium currents. *Exp. Parasitol.* **120**, 50–56. (doi:10.1016/j.exppara.2008.04.019)
63. Delgado-Ramírez M, Pottosin II, Melnikov V, Dobrovinskaya OR. 2010 Infection by *Trypanosoma cruzi* enhances anion conductance in rat neonatal ventricular cardiomyocytes. *J. Membr. Biol.* **238**, 51–61. (doi:10.1007/s00232-010-9318-6)
64. Perez S, Weis V. 2006 Nitric oxide and cnidarian bleaching: an eviction notice mediates breakdown of a symbiosis. *J. Exp. Biol.* **209**, 2804–2810. (doi:10.1242/jeb.02309)
65. Hawkins TD, Bradley BJ, Davy SK. 2013 Nitric oxide mediates coral bleaching through an apoptotic-like cell death pathway: evidence from a model sea anemone-dinoflagellate symbiosis. *FASEB J.* **27**, 4790–4798. (doi:10.1096/fj.13-235051)
66. Savitsky D, Tamura T, Yanai H, Taniguchi T. 2010 Regulation of immunity and oncogenesis by the IRF transcription factor family. *Cancer Immunol. Immunother.* **59**, 489–510. (doi:10.1007/s00262-009-0804-6)
67. Feng H, Zhang YB, Gui JF, Lemon SM, Yamane D. 2021 Interferon regulatory factor 1 (IRF1) and anti-pathogen innate immune responses. *PLoS Pathog.* **17**, e1009220. (doi:10.1371/journal.ppat.1009220)
68. Matsuyama T *et al*. 1995 Molecular cloning of LSIRF, a lymphoid-specific member of the interferon regulatory factor family that binds the interferon-stimulated response element (ISRE). *Nucleic Acids Res.* **23**, 2127–2136. (doi:10.1093/nar/23.12.2127)
69. Yamane D *et al*. 2019 Basal expression of interferon regulatory factor 1 drives intrinsic hepatocyte resistance to multiple RNA viruses. *Nat. Microbiol.* **4**, 1096–1104. (doi:10.1038/s41564-019-0425-6)
70. McCormack R, Podack ER. 2015 Perforin-2/mpeg1 and other pore-forming proteins throughout evolution. *J. Leukoc. Biol.* **98**, 761–768. (doi:10.1189/jlb.4MR1114-523RR)
71. Walters BM, Connelly MT, Young B, Traylor-Knowles N. 2020 The complicated evolutionary diversification of the mpeg-1/perforin-2 family in cnidarians. *Front. Immunol.* **11**, 1690. (doi:10.3389/fimmu.2020.01690)
72. Secombes CJ, Zou J. 2017 Evolution of interferons and interferon receptors. *Front. Immunol.* **8**, 209. (doi:10.3389/fimmu.2017.00209)
73. Lipniacki T, Paszek P, Brasier AR, Luxon BA, Kimmel M. 2006 Stochastic regulation in early immune response. *Biophys. J.* **90**, 725–742. (doi:10.1529/biophysj.104.056754)
74. Cleves PA, Krediet CJ, Lehnert EM, Onishi M, Pringle JR. 2020 Insights into coral bleaching under heat stress from analysis of gene expression in a sea anemone model system. *Proc. Natl Acad. Sci. USA* **117**, 28906–28917. (doi:10.1073/pnas.2015737117)
75. Kohchi C, Inagawa H, Nishizawa T, Soma GI. 2009 ROS and innate immunity. *Anticancer Res.* **29**, 817–821.
76. Zelko IN, Mariani TJ, Folz RJ. 2002 Superoxide dismutase multigene family: a comparison of the cuzn-SOD (SOD1), mn-SOD (SOD2), and EC-SOD (SOD3) gene structures, evolution, and expression. *Free Radic. Biol. Med.* **33**, 337–349. (doi:10.1016/s0891-5849(02)00905-x)
77. Biswas M, Chan JY. 2010 Role of Nrf1 in antioxidant response element-mediated gene expression and beyond. *Toxicol. Appl. Pharmacol.* **244**, 16–20. (doi:10.1016/j.taap.2009.07.034)
78. Yang D, Elner SG, Bian ZM, Till GO, Petty HR, Elner VM. 2007 Pro-inflammatory cytokines increase reactive oxygen species through mitochondria and NADPH oxidase in cultured RPE cells. *Exp. Eye Res.* **85**, 462–472. (doi:10.1016/j.exer.2007.06.013)
79. Marques E, Kramer R, Ryan DG. 2024 Multifaceted mitochondria in innate immunity. *NPJ Metab. Health Dis.* **2**, 6. (doi:10.1038/s44324-024-00008-3)
80. Li Y *et al*. 2019 Immune effects of glycolysis or oxidative phosphorylation metabolic pathway in protecting against bacterial infection. *J. Cell. Physiol.* **234**, 20298–20309. (doi:10.1002/jcp.28630)
81. Chaudhari N, Talwar P, Parimisetty A, Lefebvre d'Hellencourt C, Ravanan P. 2014 A molecular web: endoplasmic reticulum stress, inflammation, and oxidative stress. *Front. Cell. Neurosci.* **8**, 213. (doi:10.3389/fncel.2014.00213)
82. So JS. 2018 Roles of endoplasmic reticulum stress in immune responses. *Mol. Cells* **41**, 705–716. (doi:10.14348/molcells.2018.0241)
83. Richardson CE, Kooistra T, Kim DH. 2010 An essential role for XBP-1 in host protection against immune activation in *C. elegans*. *Nature* **463**, 1092–1095. (doi:10.1038/nature08762)
84. Chipurupalli S, Samavedam U, Robinson N. 2021 Crosstalk between ER stress, autophagy and inflammation. *Front. Med.* **8**, 758311. (doi:10.3389/fmed.2021.758311)
85. Hwang J, Qi L. 2018 Quality control in the endoplasmic reticulum: crosstalk between ERAD and UPR pathways. *Trends Biochem. Sci.* **43**, 593–605. (doi:10.1016/j.tibs.2018.06.005)
86. Kim R, Emi M, Tanabe K, Murakami S. 2006 Role of the unfolded protein response in cell death. *Apoptosis* **11**, 5–13. (doi:10.1007/s10495-005-3088-0)
87. MacKnight NJ, Dimos BA, Beavers KM, Muller EM, Brandt ME, Mydlarz LD. 2022 Disease resistance in coral is mediated by distinct adaptive and plastic gene expression profiles. *Sci. Adv.* **8**, eabo6153. (doi:10.1126/sciadv.abo6153)
88. Fuess LE, Pinzón C JH, Weil E, Grinshpon RD, Mydlarz LD. 2017 Life or death: disease-tolerant coral species activate autophagy following immune challenge. *Proc. R. Soc. B* **284**, 20170771. (doi:10.1098/rspb.2017.0771)
89. Deretic V, Saitoh T, Akira S. 2013 Autophagy in infection, inflammation and immunity. *Nat. Rev. Immunol.* **13**, 722–737. (doi:10.1038/nri3532)
90. Carrión PJA, Desai N, Brennan JJ, Fifer JE, Siggers T, Davies SW, Gilmore TD. 2023 Starvation decreases immunity and immune regulatory factor NF-κB in the starlet sea anemone *Nematostella vectensis*. *Commun. Biol.* **6**, 698. (doi:10.1038/s42003-023-05084-7)
91. Vega Thurber R *et al*. 2020 Deciphering coral disease dynamics: integrating host, microbiome, and the changing environment. *Front. Ecol. Evol.* **8**, 402. (doi:10.3389/fevo.2020.575927)
92. Emery MA, Beavers KM, Van EW, Batiste R, Dimos B, Pellegrino M *et al*. 2024 Data for: Trade-off between photo-symbiosis and innate immunity influences cnidarian's response to pathogenic bacteria. Dryad Digital Repository (doi:10.5061/dryad.02v6wwq9z)
93. Emery MA, Beavers KM, Van Buren EW, Batiste R, Dimos B, Pellegrino MW *et al*. 2024 Data from: Trade-off between photo-symbiosis and innate immunity influences cnidarian's response to pathogenic bacteria. Figshare. (doi:10.6084/m9.figshare.c.7441756)